

Optical and adsorption properties of mesoporous $\text{SiO}_2/\text{Zn}_2\text{SiO}_4:\text{Eu}^{3+}$ hollow nanospheres

Peng Dai^{1,2} ✉, You-Quan Sun², Zhi-Wei Bao¹, Jin Zhu¹, Ming-Zai Wu¹ ✉

¹School of Physics and Materials Science, Anhui University, Hefei 230601, People's Republic of China

²Anhui Deli Daily Glass Co., Ltd., Fengyang 233100, People's Republic of China

✉ E-mail: daipeng@mail.ustc.edu.cn, mingzaiwu@gmail.com

Published in Micro & Nano Letters; Received on 23rd July 2016; Revised on 26th November 2016; Accepted on 12th December 2016

Mesoporous $\text{SiO}_2/\text{Zn}_2\text{SiO}_4:\text{Eu}^{3+}$ hollow nanospheres were successfully synthesised via the combination of layer-by-layer and combustion technique. The structures and morphologies of as-obtained $\text{SiO}_2/\text{Zn}_2\text{SiO}_4:\text{Eu}^{3+}$ nanospheres were investigated using X-ray diffraction (XRD), scanning electron microscopy (SEM), transmission electron microscopy (TEM) and N_2 adsorption-desorption isotherms techniques. $\text{SiO}_2/\text{Zn}_2\text{SiO}_4:\text{Eu}^{3+}$ nanospheres can be tested as adsorbents to remove heavy metal ions, which showed good adsorption capacity and selectively adsorption especially for Pb^{2+} and Cu^{2+} than Cd^{2+} . The optical properties studies of as-synthesised samples showed that mesoporous $\text{SiO}_2/\text{Zn}_2\text{SiO}_4:\text{Eu}^{3+}$ hollow nanospheres had strong red emission around 618 nm, and the optimal loading dosage of Eu^{3+} was determined. Moreover, the mesoporous $\text{SiO}_2/\text{Zn}_2\text{SiO}_4:\text{Eu}^{3+}$ hollow nanospheres could offer cell optical imaging by conventional fluorescence with 543 nm excitation.

1. Introduction: Over the past several years, there has been a growing interest in the development of inorganic phosphors due to their wide applications in the light emitting diodes, cathode ray tubes, field emission displays, coatings in lamps and so on [1–3]. Among inorganic phosphors, Zn_2SiO_4 has been studied widely as a phosphor host material for rare earths and transition metals activators due to its excellent colour purity, luminous efficiency and chemical stability [4–6]. Particularly, $\text{Zn}_2\text{SiO}_4:\text{Eu}^{3+}$ has attracted considerable attention for its highly efficient red emission when excited by cathode rays or UV light, making it a potential material in fluorescent lamps, cathode ray tubes, lighting, plasma display panels and so on. [7–10]. Transition metals doped Zn_2SiO_4 phosphors are usually synthesised by a solid-phase reaction procedure involving long-time sintering process at high temperature and post-treatment, which usually leads to uncontrollable doped metal ions distribution, phosphor particles contamination and depression of luminescent efficiency. Thus, great efforts have been made to search for a simple and low-cost preparation method that can be easily scaled up and meet the industrial needs. Dacanin synthesised $\text{Zn}_2\text{SiO}_4:\text{Eu}^{3+}$ phosphor nanopowders with a combination of polymer-assisted sol-gel and combustion method [11]. Krsmanovic prepared $\text{Zn}_2\text{SiO}_4:\text{Eu}^{3+}$ nanophosphors with a polymer-assisted sol-gel synthesis process; while Patra got Eu^{3+} doped Zn_2SiO_4 nanoparticles with a sol-emulsion-gel method [12, 13]. Despite these achievements, it is highly demanded to synthesise $\text{Zn}_2\text{SiO}_4:\text{Eu}^{3+}$ phosphors with unique structure such as hollow cores and mesoporous shells for some practical applications including adsorption and medical imaging.

Hollow-structured mesoporous materials, as a kind of mesoporous material with unique morphology, aroused much attention in recent years due to the subtle combination of large voids and mesoporous shells. For their outstanding features such as low-density, large-specific surface area, good biocompatibility, and high permeability between outer environment and voids, they have demonstrated great potential in the fields of gene delivery, guest encapsulation, adsorption and separation, medical imaging, confined-space catalysis and so on [14–17]. Herein, we developed a layer-by-layer technique for the preparation of $\text{SiO}_2/\text{Zn}_2\text{SiO}_4:\text{Eu}^{3+}$ hollow nanospheres with mesoporous shells. The structures and morphologies of as-obtained samples were investigated in

detail. Moreover, the adsorption and optical properties including photoluminescence and optical imaging of the products were also investigated. Unique mesoporous hollow structures are believed to be responsible for the excellent optical and adsorption properties for $\text{SiO}_2/\text{Zn}_2\text{SiO}_4:\text{Eu}^{3+}$ nanospheres. To the best of our knowledge, there has been no report on the synthesis of mesoporous hollow $\text{SiO}_2/\text{Zn}_2\text{SiO}_4:\text{Eu}^{3+}$ nanospheres. Moreover, compared with the nanospheres reported in [9], the as-obtained samples have unique mesoporous hollow structures and much smaller sizes (about 110 nm), which are suitable for cell imaging.

2. Experimental details

2.1. Synthesis of mesoporous hollow $\text{SiO}_2/\text{Zn}_2\text{SiO}_4:\text{Eu}^{3+}$ nanospheres: All chemicals were of analytical grade and used without further purification. Monodisperse polystyrene spheres were fabricated based on [18, 19], and mesoporous $\text{SiO}_2/\text{Zn}_2\text{SiO}_4:\text{Eu}^{3+}$ hollow nanospheres were prepared as follows, including a layer-by-layer method and the following combustion process. In a typical synthesis, 0.1 g of monodisperse polystyrene spheres was firstly added to 25 mL of absolute ethanol with 30 min ultrasonic treatment. Secondly, 25 mL of cetyltrimethylammonium bromide solution (0.10 mol/L) and 12 mL of aqueous ammonia were introduced to the above solution. After vigorous stirring for 2 h, 0.2 g of tetraethyl orthosilicate and 0.2 g of 3-aminopropyltriethoxysilane were added dropwise. Then, 4 mL of solution including zinc acetate and europium acetate (the atom ratio of Zn:Eu is 95:5) was added with vigorously stirring at room temperature for 10 h. Then the mixed solution was transferred into a 50 autoclave with a Teflon liner, keeping at 80°C for 48 h. The products were rinsed thoroughly with absolute ethanol and distilled water, and dried at 50°C for 12 h. Thus, the extracted mesoporous $\text{SiO}_2/\text{Zn}_2\text{SiO}_4:\text{Eu}^{3+}$ hollow nanospheres were obtained by eliminating the templates and surfactants under calcinations at 850°C for 5 h in a muffle oven, which is labelled sample S1. Samples S2 and S3 were synthesised through the same procedure with different atom ratio of Zn to Eu, in which are Zn:Eu = 92:8 and Zn:Eu = 90:10, respectively. In addition, $\text{Zn}_2\text{SiO}_4:\text{Eu}^{3+}$ nanoparticles were also fabricated based on [13] for comparative study of optical properties, and labelled as sample S0, in which Zn:Eu = 92:8.

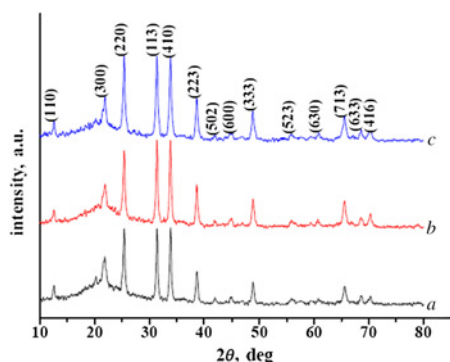


Fig. 1 The XRD patterns of samples S1, S2 and S3

2.2. Characterisation of the samples: The phase compositions of products were determined by an 18 kW advanced XRD (Briler D8-ADVANCE) with a $\text{Cu K}\alpha$ line of 1.54056 Å. The morphologies of the synthesised samples were observed using SEM (S-4800, Hitachi, Japan) and TEM (JEM-2100, JEOL, Japan). Specific surface areas were calculated by the Barrett–Emmett–Teller (BET) method (3H-2000PS2, BeiShiDe Instrument, China). The photoluminescent emission spectra were measured by a fluorescence spectrometer with scanning rate of 60 nm/min (F-4500, Shimadzu, Japan). The adsorption capacities for heavy metal ions were tested by inductively coupled plasma atomic emission spectroscopy (ICPE-9000, Shimadzu, Japan).

3. Results and discussion: Fig. 1 shows the XRD patterns for samples S1, S2 and S3 annealed at 850°C. All samples have similar diffraction peaks and can be well indexed to willemite zinc silicate (JCPDS Card No. 37-1485). The broad peak at about 22° is the characteristic peak for amorphous SiO_2 (JCPDS Card No. 29-0085), which suggests that some silica still exist in the as-obtained samples. Furthermore, no diffraction peaks of europium oxide or compounds are detected, indicating Eu ions are completely dissolved into the lattice of zinc silicate.

The morphologies and microstructures of samples S1, S2 and S3 were further investigated by SEM and TEM micrographs in Fig. 2. Fig. 2a shows the SEM images of polystyrene (PS) nanospheres, which have highly even size distribution. The average particle size is about 100 nm in diameter. After the layer-by-layer coating, core-shell structures with diameter about 110 nm are formed before heat treatment, as shown in the circled area in Fig. 2b. The size increase of core-shell-structured nanospheres can be easily understood due to the coating of SiO_2 and $\text{Zn}(\text{OH})_2$ onto the PS nanospheres core during the process of hydrolysis and condensation. After the annealing treatment, many pores are scattered on the shells, confirming the formation of mesoporous shell, as shown in Fig. 2c. To confirm the presence of Eu in phosphors, energy dispersive spectrometry (EDS) analysis was performed (Fig. 2d). It is clear that the as-synthesised samples are composed of Zn, Si, O, Eu and C, which indicates the doping of Eu^{3+} into the lattice of Zn_2SiO_4 . Fig. 2e further gives TEM image of sample S2. The dark edge and the pale centre indicate the existence of the hollow nature for the nanospheres. The average size of cavities is approximately 95 nm, and the thickness of shells is about 8.5 nm. Moreover, the well-ordered lattice fringes in Fig. 2f is calculated to be 0.26 nm, which can be ascribed to the (410) crystal plane of Zn_2SiO_4 .

To characterise the porosity and specific surface areas of $\text{SiO}_2/\text{Zn}_2\text{SiO}_4:\text{Eu}^{3+}$ nanospheres, nitrogen adsorption–desorption experiments were adopted. In Fig. 3a, sample S2 shows typical type IV isotherms with a type H3 hysteresis loop, indicating the mesoporous nature of the shell in $\text{SiO}_2/\text{Zn}_2\text{SiO}_4:\text{Eu}^{3+}$ hollow nanospheres [20, 21]. Fig. 3b shows the pore size distribution curve calculated

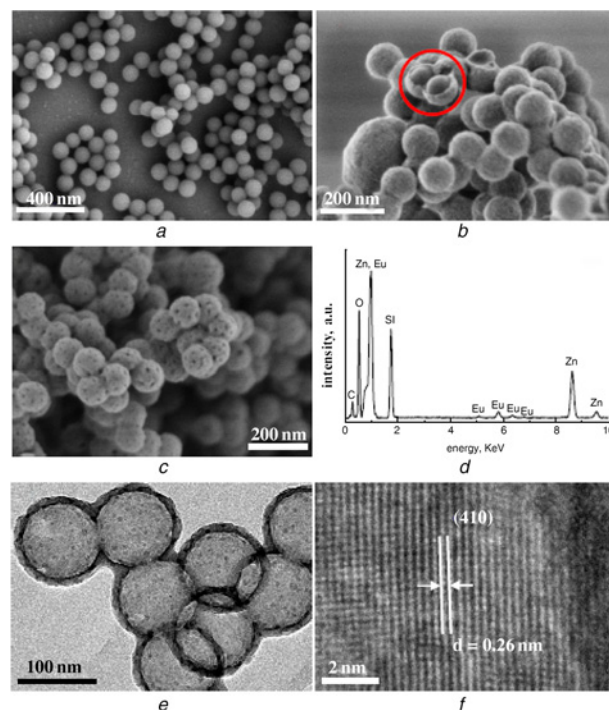


Fig. 2 SEM @ TEM micrographs of as-obtained samples

- a SEM micrographs of PS microspheres
- b SEM micrographs of composite spheres without heat treatment
- c SEM micrographs of sample S2
- d EDS spectrum of sample S2
- e TEM micrographs of sample S2
- f HRTEM micrographs of sample S2

by Barrett–Joyner–Halenda (BJH) method according to the adsorption branch of the isotherm. There is a peak with pore diameter of around 6.7 nm, and the BET surface area and a pore volume can be calculated as 232.4 m^2/g and 0.31 cm^3/g , respectively. Therefore, it is suggested that the as-synthesised samples have unique structure of the nanospheres with mesopore walls and the hollow cavities.

It has been reported that nano-structured hollow spheres possessed superior adsorption capacities of removing heavy metal ions [14, 22]. In this study, the ability of removal of heavy metal ions of $\text{SiO}_2/\text{Zn}_2\text{SiO}_4:\text{Eu}^{3+}$ nanospheres was also examined, as shown in Table 1. Based on [19], the adsorption and metal ion removal capabilities of phosphors were mainly dependent on the mesoporous $\text{SiO}_2/\text{Zn}_2\text{SiO}_4$ hollow structures. Thus, sample S2 was selected to perform the adsorption and metal ion removal capabilities. In a typical process, sample S2 (about 50 mg in dry weight) was incubated in the respective 20 mL aqueous solutions with initial concentrations of 200 mg/L containing Pb^{2+} , Cu^{2+} and Cd^{2+} . The pH values of these solutions were adjusted to 2 with dilute HCl to prevent heavy metal ions hydrolysing. After being vigorously stirred for 3 h, the mixtures are centrifuged to have inductively coupled plasma

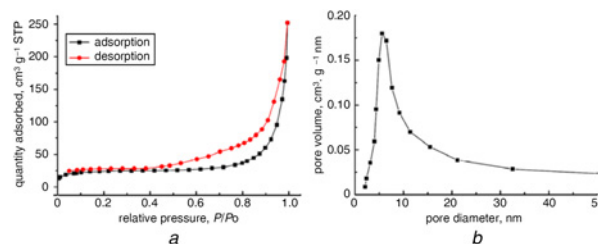


Fig. 3 Nitrogen physisorption isotherms of sample S2

- a N2 adsorption–desorption isotherms
- b Corresponding pore size distribution curves

Table 1 Capacities of SiO₂/Zn₂SiO₄:Eu³⁺ nanospheres for removal of metal ions

Ions	Initial concentration, mg/L	Final concentration, mg/L	Absorption amount, mg/g
Pb ²⁺	200	3.85	78.46
Cu ²⁺	200	18.55	72.58
Cd ²⁺	200	83.575	46.57

atomic emission spectroscopy test. It is clear that the adsorption capacity for Pb²⁺, Cu²⁺ and Cd²⁺ of sample S2 are 78.46, 72.58 and 46.57 mg/g, respectively. Noteworthy, sample S2 exhibits good adsorption capacity and selectively adsorption especially for Pb²⁺ and Cu²⁺, which can be ascribed to its large surface area and unique mesoporous hollow structure.

The luminescence of SiO₂/Zn₂SiO₄:Eu³⁺ nanospheres was investigated. Fig. 4 shows the room temperature photoluminescence emission spectra of samples with different Eu³⁺ concentration. It can be seen obviously that upon excitation at 395 nm, all the samples indicate sharp emission bands with the same positions. The emission peaks at about 594, 618, 654 and 703 nm are the typical emission bands of Eu³⁺ in zinc silicate and can be assigned to the electronic transitions ⁵D₀→⁷F₁, ⁵D₀→⁷F₂, ⁵D₀→⁷F₃ and ⁵D₀→⁷F₄, respectively [9, 10]. For the ⁵D₀→⁷F₁ transition, it is a parity-allowed magnetic-dipole transition and the intensity is independent of the site symmetry at which europium is situated. For ⁵D₀→⁷F₂ transition, it is a hypersensitive forced electric-dipole transition, whose intensity is relevant with the symmetry of the crystal field around Eu³⁺. Hence, each electronic transition is dependent on different factor. With the increase of Eu³⁺ concentration from sample S1 (5%) to S3 (10%), the emission intensities of the four peaks do not show proportional changes. Moreover, samples S1, S2 and S3 show intense red emission at about 618 nm, and sample S2 has the highest emission intensity. With increase in the doping concentration of Eu³⁺ from sample S1 (5%) to S2 (8%), more radiative Eu³⁺ states located in zinc silicate will lead to the increase of emission intensities. However, when the doping concentration of Eu³⁺ is further increased from sample S2 (8%) to S3 (10%), the emission intensity decreases, which can be ascribed to concentration quenching effect of Eu³⁺ [9]. Therefore, there exists an optimal doping of Eu³⁺ for the highest emission intensity. In addition, as an industry standard, commercial red phosphor (Y₂O₃:Eu, MaTeck GmbH) was chosen for the comparative study. In Fig. 4, sample S2 has about 95% photoluminescence intensity of commercial phosphor, and sample S3 also has about 75% emission intensity of commercial phosphor, indicating the excellent photoluminescent properties of as-obtained SiO₂/Zn₂SiO₄:Eu³⁺ phosphors.

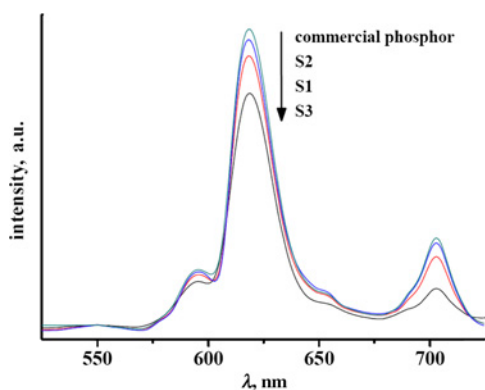


Fig. 4 Room temperature emission spectra of samples S1, S2, S3 and commercial phosphor under 395 nm excitation

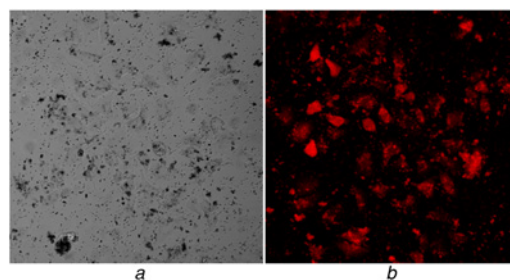


Fig. 5 Confocal laser scanning microscopy images of sample S2
a In bright field
b Excited with 543 nm laser beams

To study the optical imaging properties of SiO₂/Zn₂SiO₄:Eu³⁺ nanospheres, sample S2 was cultivated with human cervical carcinoma (HeLa) cells seeded onto sterile and acid-treated 12 mm coverslips in 24-well plates for 24 h, and then laser scanning microscopy test was performed by confocal laser scanning microscope (Zeiss LSM 710, 543 nm/1.2 mw) without any further dyeing. It can be seen in Fig. 5, SiO₂/Zn₂SiO₄:Eu³⁺ nanospheres could be devoured by cells and were localised in cytoplasm, and red fluorescence signals can be observed when excited under the wavelength of 543 nm. It is suggested that the fluorescence signals are from SiO₂/Zn₂SiO₄:Eu³⁺ nanospheres due to the fact that HeLa cells were not disposed with dyeing. Therefore, SiO₂/Zn₂SiO₄:Eu³⁺ nanospheres have high-potential towards applications in bio-imaging and bio-labelling.

4. Conclusion: In summary, mesoporous SiO₂/Zn₂SiO₄:Eu³⁺ hollow nanospheres are fabricated via a layer-by-layer method and the following combustion process. The structures and morphologies of as-obtained samples are examined in detail, and the results confirmed the existence of mesoporous hollow structures in SiO₂/Zn₂SiO₄:Eu³⁺ nanospheres. The products perform excellent heavy metal adsorption capacity of 78.46, 72.58 and 46.57 mg/g for Pb²⁺, Cu²⁺ and Cd²⁺, respectively. Meanwhile, they show intense red emission at about 618 nm, and only proper Eu³⁺ loading in SiO₂/Zn₂SiO₄:Eu³⁺ nanospheres can get the highest photoluminescence emission intensity. Moreover, upon incubation with HeLa cells, the intrinsic luminescence of SiO₂/Zn₂SiO₄:Eu³⁺ nanospheres show the function of optical imaging, suggesting the potential towards applications in cell imaging.

5. Acknowledgments: This Letter was financially supported by National Natural Science Foundation of China (grant nos. 51502002, 11374013 and 51672001), Provincial Science Foundation of Anhui (grant no. 1608085ME97).

6 References

- [1] Li G.G., Tian Y., Zhao Y., *ET AL.*: 'Recent progress in luminescence tuning of Ce³⁺ and Eu²⁺-activated phosphors for pc-WLEDs', *Chem. Soc. Rev.*, 2015, **44**, (23), pp. 8688–8713
- [2] Pust P., Schmidt P.J., Schnick W.: 'A revolution in lighting', *Nat. Mater.*, 2015, **14**, (5), pp. 454–458
- [3] Li G.G., Lin J.: 'Recent progress in low-voltage cathodoluminescent materials: synthesis, improvement and emission properties', *Chem. Soc. Rev.*, 2014, **43**, (20), pp. 7099–7131
- [4] Zhang S.Y., Hou L.L., Hou M.H., *ET AL.*: 'Hydrothermal synthesis of spindle-like Zn₂SiO₄ nanoparticles and its application in lithium-ion battery', *Mater. Lett.*, 2015, **156**, pp. 82–85
- [5] Wen C.W., Yong T.T., Kun L., *ET AL.*: 'Capacitive humidity-sensing properties of Zn₂SiO₄ film grown on silicon nanoporous pillar array', *Appl. Surf. Sci.*, 2013, **273**, pp. 372–376
- [6] Zhang S.Y., Ren L., Peng S.J.: 'Zn₂SiO₄ urchin-like microspheres: controlled synthesis and application in lithium-ion batteries', *CrystEngComm*, 2014, **16**, (27), pp. 6195–6202

- [7] Basavaraj R.B., Nagabhushana H., Daruka Prasad B., *ET AL.*: 'A single host white light emitting $\text{Zn}_2\text{SiO}_4\text{:Re}^{3+}(\text{Eu, Dy, Sm})$ phosphor for LED applications', *Optik*, 2015, **126**, (19), pp. 1745–1756
- [8] Ramakrishna P.V., Murthy D.B.R.K., Sastry D.L.: 'White-light emitting Eu^{3+} co-doped $\text{ZnO/Zn}_2\text{SiO}_4\text{:Mn}^{2+}$ composite microphosphor', *Spectrochim. Acta A*, 2014, **125**, pp. 234–238
- [9] Wu Y., Wang Y.S., He D.W., *ET AL.*: 'Spherical $\text{Zn}_2\text{SiO}_4\text{:Eu}^{3+}/\text{SiO}_2$ phosphor particles in core-shell structure: synthesis and characterization', *J. Lumin.*, 2010, **130**, (10), pp. 1768–1773
- [10] Joly A.G., Chen W., Zhang J., *ET AL.*: 'Electronic energy relaxation and luminescence decay dynamics of Eu^{3+} in $\text{Zn}_2\text{SiO}_4\text{:Eu}^{3+}$ phosphors', *J. Lumin.*, 2007, **126**, (2), pp. 491–496
- [11] Dacanin L., Lukic S.R., Petrovic D.M., *ET AL.*: 'Judd-Ofelt analysis of luminescence emission from $\text{Zn}_2\text{SiO}_4\text{:Eu}^{3+}$ nanoparticles obtained by a polymer-assisted sol-gel method', *Physica B*, 2011, **406**, (11), pp. 2319–2322
- [12] Krsmanovic R., Antic Z., Zekovic I., *ET AL.*: 'Polymer-assisted sol-gel synthesis and characterization of $\text{Zn}_2\text{SiO}_4\text{:Eu}^{3+}$ powders', *J. Alloy. Compd.*, 2009, **480**, (2), pp. 494–498
- [13] Patra A., Baker G.A., Baker S.N.: 'Synthesis and luminescence study of Eu^{3+} in Zn_2SiO_4 nanocrystals', *Opt. Mater.*, 2004, **27**, (1), pp. 15–20
- [14] Li Y.S., Shi J.L.: 'Hollow-structured mesoporous materials: chemical synthesis, functionalization and applications', *Adv. Mater.*, 2014, **26**, (20), pp. 3176–3205
- [15] Pan J.H., Wang X.Z., Huang Q.Z., *ET AL.*: 'Large-scale synthesis of urchin-like mesoporous TiO_2 hollow spheres by targeted etching and their photoelectrochemical properties', *Adv. Funct. Mater.*, 2014, **24**, (1), pp. 95–104
- [16] Liu C., Wang J., Li J.S., *ET AL.*: 'Synthesis of N-doped hollow-structured mesoporous carbon nanospheres for high-performance supercapacitors', *ACS Appl. Mater. Interfaces*, 2016, **8**, (11), pp. 7194–7204
- [17] Shen J., Song G.S., An M., *ET AL.*: 'The use of hollow mesoporous silica nanospheres to encapsulate bortezomib and improve efficacy for non-small cell lung cancer therapy', *Biomaterials*, 2014, **35**, (1), pp. 316–326
- [18] Xu Z.M., Wang Y.X.: 'Hollow $\text{ZnO/Zn}_2\text{SiO}_4/\text{SiO}_2$ sub-microspheres with mesoporous shells: synthesis, characterization, adsorption and photoluminescence', *J. Alloys Compd.*, 2013, **555**, pp. 268–273
- [19] Dai P., Xu Z.M., Yu X.X., *ET AL.*: 'Mesoporous hollow $\text{Zn}_2\text{SiO}_4\text{:Mn}^{2+}$ nanospheres: the study of photoluminescence and adsorption properties', *Mater. Res. Bull.*, 2014, **61**, pp. 76–82
- [20] Sing K.S.W., Everett D.H., Haul R.A.W., *ET AL.*: 'Reporting physiosorption data for gas/solid systems with special reference to the determination of surface area and porosity', *Pure Appl. Chem.*, 1985, **57**, (11), pp. 603–619
- [21] Tompsett G.A., Krogh L., Griffin D.W., *ET AL.*: 'Hysteresis and scanning behavior of mesoporous molecular sieves', *Langmuir*, 2005, **21**, (18), pp. 8214–8225
- [22] Zhang X., Wu T.X., Zhang Y.X., *ET AL.*: 'Adsorption of Hg^{2+} by thiol functionalized hollow mesoporous silica microspheres with magnetic cores', *RSC Adv.*, 2015, **5**, (63), pp. 51446–51453